Practical Aspects of novel MRI Techniques in Neuroradiology: Part 1 – 3D Acquisitions, Dixon Techniques and Artefact Reduction

Praktische Aspekte neuerer MRT-Techniken in der Neuroradiologie: Teil 1 – 3D, Dixon-Techniken und Artefaktreduktion

Authors

Benedikt Sundermann[1, 2, 3], Benoit Billebaut[3, 4], Jochen Bauer[3], Catalin George Iacoban[1], Olga Alykova[1], Christoph Schülke[5], Maike Gerdes[1], Harald Kugel[3], Sojan Neduvakkattu[3], Holger Bösenberg[1], Christian Mathys[1, 2, 6]

Affiliations

1 Institute of Radiology and Neuroradiology, Evangelisches Krankenhaus, Medical Campus University of Oldenburg, Germany
2 Research Center Neurosensory Science, University of Oldenburg, Germany
3 Clinic for Radiology, University Hospital Münster, Germany
4 School for Radiologic Technologists, University Hospital Münster, Germany
5 Radiologie Salzstraße, Münster, Germany
6 Department of Diagnostic and Interventional Radiology, University of Düsseldorf, Germany

Key words

MR-imaging, neuroradiology, 3D imaging, metal artefact reduction, movement artefact reduction, Dixon

received 31.08.2021
accepted 05.03.2022
published online 11.05.2022

Bibliography

Fortschr Röntgenstr 2022; 194: 1100–1108
DOI 10.1055/a-1800-8692
ISSN 1438-9029

Georg Thieme Verlag KG, Rüdigerstraße 14, 70469 Stuttgart, Germany

Correspondence

PD Dr. Benedikt Sundermann
Institut für Radiologie und Neuroradiologie, Evangelisches Krankenhaus Oldenburg, Steinweg 13–17, 26122 Oldenburg, Germany
Tel.: +49/4 41/2 36 97 54
benedikt.sundermann@uni-oldenburg.de

Supplementary material is available under https://doi.org/10.1055/a-1800-8692

ABSTRACT

Background Recently introduced MRI techniques offer improved image quality and facilitate examinations of patients even when artefacts are expected. They pave the way for novel diagnostic imaging strategies in neuroradiology. These methods include improved 3D imaging, movement and metal artefact reduction techniques as well as Dixon techniques.

Methods Narrative review with an educational focus based on current literature research and practical experiences of different professions involved (physicians, MRI technologists/radiographers, physics/biomedical engineering). Different hardware manufacturers are considered.

Results and Conclusions 3D FLAIR is an example of a versatile 3D Turbo Spin Echo sequence with broad applicability in routine brain protocols. It facilitates detection of smaller lesions and more precise measurements for follow-up imaging. It also offers high sensitivity for extracerebral lesions. 3D techniques are increasingly adopted for imaging arterial vessel walls, cerebrospinal fluid spaces and peripheral nerves. Improved hybrid-radial acquisitions are available for movement artefact reduction in a broad application spectrum. Novel susceptibility artefact reduction techniques for targeted application supplement previously established metal artefact reduction sequences. Most of these techniques can be further adapted to achieve the desired diagnostic performances. Dixon techniques allow for homogeneous fat suppression in transition areas and calculation of different image contrasts based on a single acquisition.

Key points:

- 3D FLAIR can replace 2 D FLAIR for most brain imaging applications and can be a cornerstone of more precise and more widely applicable protocols.
- Further 3D TSE sequences are increasingly replacing 2D TSE sequences for specific applications.
- Improvement of artefact reduction techniques increase the potential for effective diagnostic MRI exams despite movement or near metal implants.
- Dixon techniques facilitate homogeneous fat suppression and simultaneous acquisition of multiple contrasts.

Citation Format

- Sundermann B, Billebaut B, Bauer J et al. Practical Aspects of novel MRI Techniques in Neuroradiology: Part 1 – 3D Acquisitions, Dixon Techniques and Artefact Reduction. Fortschr Röntgenstr 2022; 194: 1100–1108

ZUSAMMENFASSUNG

Hintergrund Neuere MR-Techniken ermöglichen es, gestiegene Anforderungen an Bildqualität zu erfüllen, Patienten trotz zu erwartender Artefakte zu untersuchen und neue Untersuchungsstrategien in der Neuroradiologie zu entwickeln. Dies sind unter anderem verbesserte 3D-Techniken, Methoden zur Verminderung von Bewegungs- und Metall-Artefakten und Dixon-Techniken.

Methode Narrative Übersichtsarbeit mit Fortbildungsschwerpunkt basierend auf aktueller Literaturrecherche und praktischen Erfahrungen verschiedener Berufsgruppen (ärztliches Personal, MTRA, MR-Physik/Technik) und mit Geräten unterschiedlicher Hersteller.

Ergebnisse und Schlussfolgerungen Unter den 3D-Turbo-Spin-Echo-Techniken fällt insbesondere die 3D FLAIR-Sequenz durch vielfältige Einsatzmöglichkeiten in Routineprotokollen auf. Neben der Erkennbarkeit kleinerer Läsionen ermöglicht sie eine präzisere Verlaufsbeurteilung und eine gute Erkennbarkeit auch extrazerebraler Läsionen. 3D-Sequenzen sind zunehmend etabliert zur Beurteilung arterieller Gefäßwände, der Liquorräume und peripherer Nerven. Weiterentwickelte hybrid-radiale Sequenzen ermöglichen ein breiteres Anwendungsspektrum zur Vermeidung von Bewegungsartefakten. Für die Verringerung von Suszeptibilitätsartefakten stehen nun mehrere unterschiedliche Optionen zur Verfügung, die möglichst gezielt eingesetzt werden sollten. Die neuen Techniken ermöglichen zum Teil gezielte Anpassungen zur Erzielung der gewünschten diagnostischen Aussagefähigkeit. Dixon-Techniken ermöglichen es, über eine homogene Fettsättigung in Übergangsregionen hinaus, mit einer Messung mehrere Bildkontraste zu erzielen.

Introduction

New generations of equipment have enabled techniques in magnetic resonance imaging (MRI) to achieve clinical application maturity. They are fundamentally changing current imaging strategies. These include 3D techniques, new acceleration methods, artefact reduction procedures as well as possible combinations thereof. This is also reflected in international consensus recommendations for common diseases [1–6]. As users, we would like to[1] explain the technical background of these procedures in an understandable way and share experiences[2] from clinical use. Therefore we are focusing on those MRI techniques that are currently in transition to, or are particularly suitable for, broad routine use. Please refer to specific literature for advanced imaging techniques which are reserved for special indications [7]. The second part of this review provides an outlook covering promising techniques that are still preclinical or at the beginning of clinical use. The first part describes 3D, Dixon and artefact reduction techniques; the second part mainly presents new acceleration techniques and applications for different body regions. We have separately identified suitable further review literature with a methodological focus that illustrates the techniques presented in more detail.

Techniques

3D Techniques

3D acquisition techniques refer to the acquisition of a volume data set with near isotropic resolution instead of individual slices. While in conventional 2 D multislice imaging, slices are excited individually and the slice thickness is typically much larger than the edge length of the pixels in the slice plane, a thick slab is excited during 3D imaging, which is resolved into individual slices by a second phase encoding. This allows much higher spatial resolution in this third spatial direction; likewise isotropic voxels are possible [8]. 3D methods are suitable when lesions are to be measured reproducibly during their progression, when their positional relationship to neighboring structures is to be precisely determined and when the distribution pattern of multiple lesions is to be characterized. They are thus a prerequisite for a structured follow-up of lesions independent of primary slice angulation and allow the employment of advanced image analysis techniques including image registration and artificial intelligence. In addition, they are used for intraoperative navigation, for example. They offer the advantage of multiplane reconstructions for visual diagnosis.

3D Turbo Spin Echo (TSE)

The acquisition of a large volume with higher resolution is usually unrealistic when using “conventional” 3D TSE techniques due to a long measurement time and a high specific absorption rate (SAR). The reason for this in conventional TSE techniques [9] is the numerous 180° refocusing pulses. New modified 3D TSE techniques [8] address these problems by designing long echo trains (high turbo factor) with variable lower refocusing angles. The sequence of refocusing angles is chosen in such a way that the resulting image contrast is similar to that when using multiple 180° pulses. Contrast here is mainly based on stimulated echoes [8]. It is important to observe the contrast-related “effective” echo time when changing the sequence parameters [8]. In addition, these sequences use short, spatially non-selective high frequency pulses which allow a short echo interval, and thus enable the long echo trains required for the acquisition of a large volume in clinically acceptable measurement time [8]. In addition, these methods employ acceleration techniques such as optimized parallel ima-

1 For better readability, this article uses the generic masculine where appropriate. All personal designations apply equally to all genders.

2 In addition to scientific evidence, this article includes, to a lesser extent, descriptions of the authors' practical experiences in areas where no scientific literature is available.

ging [8] or compressed sensing (CS, see Part 2). Manufacturer designations[3] of such techniques include CUBE, VIEW/VISTA and SPACE. Improvements in homogeneity and measurement time have increasingly established these modified 3D TSE techniques as routine clinical procedures, e. g., 3D Fluid Attenuated Inversion Recovery (FLAIR). Further reading: [8]

T2 FLAIR 3D

Technical background and potential advantages

FLAIR is the primary examination technique for the detection and follow-up of cerebral lesions, e. g., in multiple sclerosis [1–3]. The higher resolution and reformatting capability are the main advantages of 3D FLAIR over 2 D FLAIR for this application. The basic principle of the underlying 3D TSE sequences with variable refocusing angles is described in the previous section. Since 3D FLAIR techniques with low refocusing angle lead to pronounced flow-related signal cancellations (flow voids) [8] while at the same time are hardly affected by hyperintense flow artefacts [10, 11], they can also be used more widely outside the brain parenchyma than 2 D FLAIR, partly even for the assessment of venous vessels (▶ **Fig. 1**). 3D FLAIR sequences appear to be relatively less susceptible to motion artefacts compared to conventional 2D Cartesian TSE sequences. In this case, moderate motion effects do not lead to multiple contours or ghost images in phase encoding direction, but rather to a relatively small increase in overall image blur.

Combined with fat suppression, 3D FLAIR could achieve possible additional diagnostic information about extracranial or bony lesions in primary cerebral examination protocols without increasing measurement time. Thus, 3D FLAIR is suitable as a cross-indication replacement for 2 D FLAIR sequences in most cases, and contributes to the reduction of the number of indication-specific brain MRI examination protocols due to its independence from slice orientation. Further reading: [12]

Possible limitations

Limitations of 3D FLAIR compared to 2 D FLAIR have only been described in a few indications (e. g., detection of the so-called “ivy sign” in moyamoya disease [13]). Despite overall low susceptibility, motion artefacts can sometimes appear as signal fluctuations (▶ **Fig. 2**), mimicking cortical lesions, for example. In 3 T, significant signal inhomogeneities may occur in older scanners due to B1 inhomogeneities [7], through which, for example, the temporal lobes appear differently bright. For example, this may affect the assessability of autoimmune encephalitis. To the best of our knowledge, there are no direct possibilities for the user to influence this by selecting measurement parameters. The respective implementation of the sequence can have an influence and, if necessary, a 2 D FLAIR is preferable to a 3D sequence.

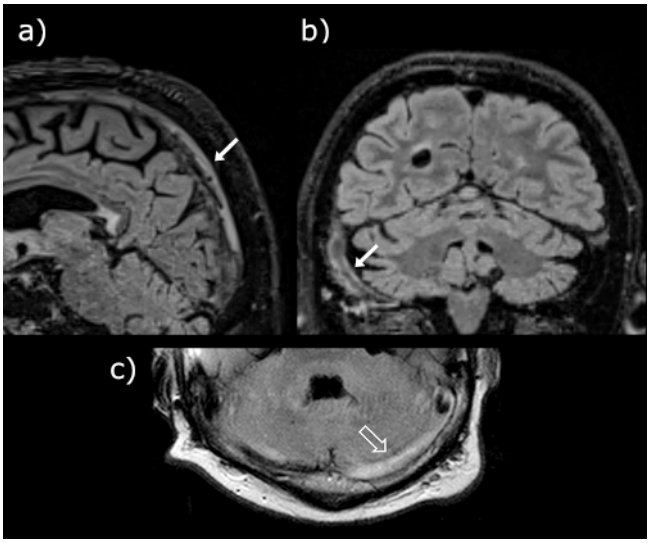

▶ **Fig. 1** 3D FLAIR in two different patients with venous sinus thrombosis: **a** superior sagittal sinus, subacute stage; **b** sigmoid sinus, acute stage. The thrombus leads to a lack of typical flow void in the corresponding sinus (arrows). 3D FLAIR, compared with **c** 2D FLAIR, is less susceptible to hyperintense flow related artefacts (open arrow). However, such artefacts should be considered in narrow vessel segments. Final assessment should take all available sequences into account since a thrombus can be totally T2 hypointense in rare cases.

Practical notes on application

▶ **Fig. 3** summarizes geometric aspects that can contribute to the avoidance of artefacts and the more efficient use of 3D FLAIR in practical routine use. The sequences provided by the manufacturers have a good contrast-to-noise ratio (CNR) for many lesion types. Originally, the signal-to-noise ratio (SNR) was often the determining factor for the presets. For example, while a sequence with a longer repetition time (TR) typically leads to a reduction in SNR due to the resulting further setting adjustments required, the CNR for lesions initially increases within a certain range [14, 15]. Therefore, for example, protocol recommendations for gliomas [4] call for a TR of 6000 to 10 000 ms. This is sometimes not compatible with acceptable measurement time in older implementations. When combined with newer acceleration techniques, these recommendations can be fully implemented. A suitable combination of repetition time (TR), (effective) echo time (TE) and inversion time (TI) is required to achieve complete suppression of the CSF signal [12]. Since no good heuristic exists for determining their appropriate ratio, it is recommended here to select these parameters based on different presets or published combinations (e. g., considering the field strength [14, 16]) instead of freely varying them. Since the subjective image impression of 3D FLAIR differs from that of 2 D FLAIR sequences, a familiarization phase is useful for reliable diagnosis.

3 In some instances trade names are provided in this article for user orientation because there is no uniform non-proprietary name concept for MR techniques as in pharmacology. In contrast to other abbreviations, acronyms which primarily have the character of a product or proper name are not listed here for better readability. Some of these are trademarks of the respective manufacturers. The naming also partly reflects the practical experiences of the authors. In particular, designation is not intended to give preference to any specific manufacturer and its implementations, nor to infringe upon any corresponding trademark rights.

▶ **Fig. 2** 3D FLAIR (accelerated by compressed sensing) in a patient with moderate movement artefacts. Movement can lead to small-scale signal fluctuations in this technique. This might imitate cortical lesions (examples highlighted by arrows) if the reader is not aware of this artefact.

Examples of further 3D TSE techniques

The high flow void susceptibility of 3D TSE sequences can be used in a targeted manner with a reduced refocusing angle, and thus capture certain flow phenomena with T2-weighted sequences [17]. However, T2-weighted 3D TSE sequences without CSF suppression have not yet been accepted as a full-fledged substitute for 2 D T2 sequences of the brain. They exhibit altered parenchymal contrast due to the long echo trains and magnetization transfer effects of the refocusing pulses [8]. They are also susceptible to truncation artefacts [18]. T2 TSE sequences are commonly used for visual classification of anatomical details and assessment of lesion morphology for which a high in-plane resolution can be advantageous, as primarily offered by 2 D sequences.

T1-weighted fat-suppressed TSE 3D sequences have recently become the standard for vessel wall imaging [19, 20] and have increasingly replaced 2 D "black blood" techniques. This is based on the pronounced flow void of these sequences [8]. Although initially described at 7.0 T and 3.0 T [19], based on the authors' experience image quality can also be achieved with current 1.5 T devices which exceed the informative capability of comparable 2 D techniques (for example parameters see **Online Table 1**). Our experience shows that basic settings do not always meet diagnostic requirements. Special attention should be paid to a resolution in the sub-millimeter range (if necessary with the aid of compressed sensing) [21–24] and sufficient suppression of flowing blood (if necessary with additional techniques such as a prepulse [25] and/or lowering of the refocusing angle [8, 19]). Further reading: [19] These T1-weighted sequences have a good contrast-to-noise ratio for barrier-disrupted lesions when imaging the brain parenchyma. Nevertheless, these sequences can also provide good co-assessment of extracranial structures [26]. However, artefacts sometimes occur due to slow flow in superficial veins [19] and field strength-dependent differences in image impression.

3D Gradient Echo

3D gradient echo techniques have been in routine clinical use for some time and will therefore not be discussed in depth here. Examples include T1-weighted sequences with inversion prepulse (e. g. MPRAGE [27]) and susceptibility-weighted imaging (SWI) [28, 29]. Due to higher sensitivity and specificity, SWI has largely replaced T2*-weighted 2 D sequences for brain imaging for appropriate indications. In this case, we recommend reconstruction of phase images [29] for a more specific assessment. Further references for SWI: [29]. Innovations in 3D gradient-echo sequences have arisen most recently from the combination possibilities with Dixon [30] and newer acceleration techniques [31, 32].

Artefact Reduction Techniques

Radial Sampling Techniques

Technical background and potential advantages

Techniques to reduce motion artefacts in 2 D sequences are widely used clinically under names such as PROPELLER [33], MultiVANE, JET, RADAR, and BLADE [34–39]. They are based on the acquisition of Cartesian-acquired segments of k-space with only a few phase encoding steps where the segments are arranged like spokes of a wheel (radial-Cartesian trajectory hybrids). The center of the k-space is captured by each spoke. Analysis of the difference between the averaged signals and the individual signals of each spoke in the center enables correction of movements in the slice plane, including both translation and rotation, and to a certain extent also movements in the slice direction [33]. Artefacts in sequences with radial scanning, e. g., due to residual aliasing, often appear in the form of radially arranged stripes. This image impression is also caused by "gridding", i. e. the projection of the radially recorded points in k-space onto the points of a Cartesian matrix, which is then Fourier-transformed to obtain the image. Such artefacts [39, 40] are usually perceived as less disturbing for the findings than motion artefacts with purely Cartesian sampling. Recently, motion corrections have been improved by newer iterative methods [41]. The basic principle of combining partial radial sequences with motion correction has now been applied to T1-weighted 3D gradient echo sequences. Examples include techniques such as StarVIBE [42–45] and radial eTHRIVE [46]. In our experience, robust and low-artefact image quality can be achieved with these sequences over many patients. Further reading: [39]

Possible limitations

With respect to comparable purely Cartesian techniques, the spatial resolution achievable in realistic measurement time is lower.

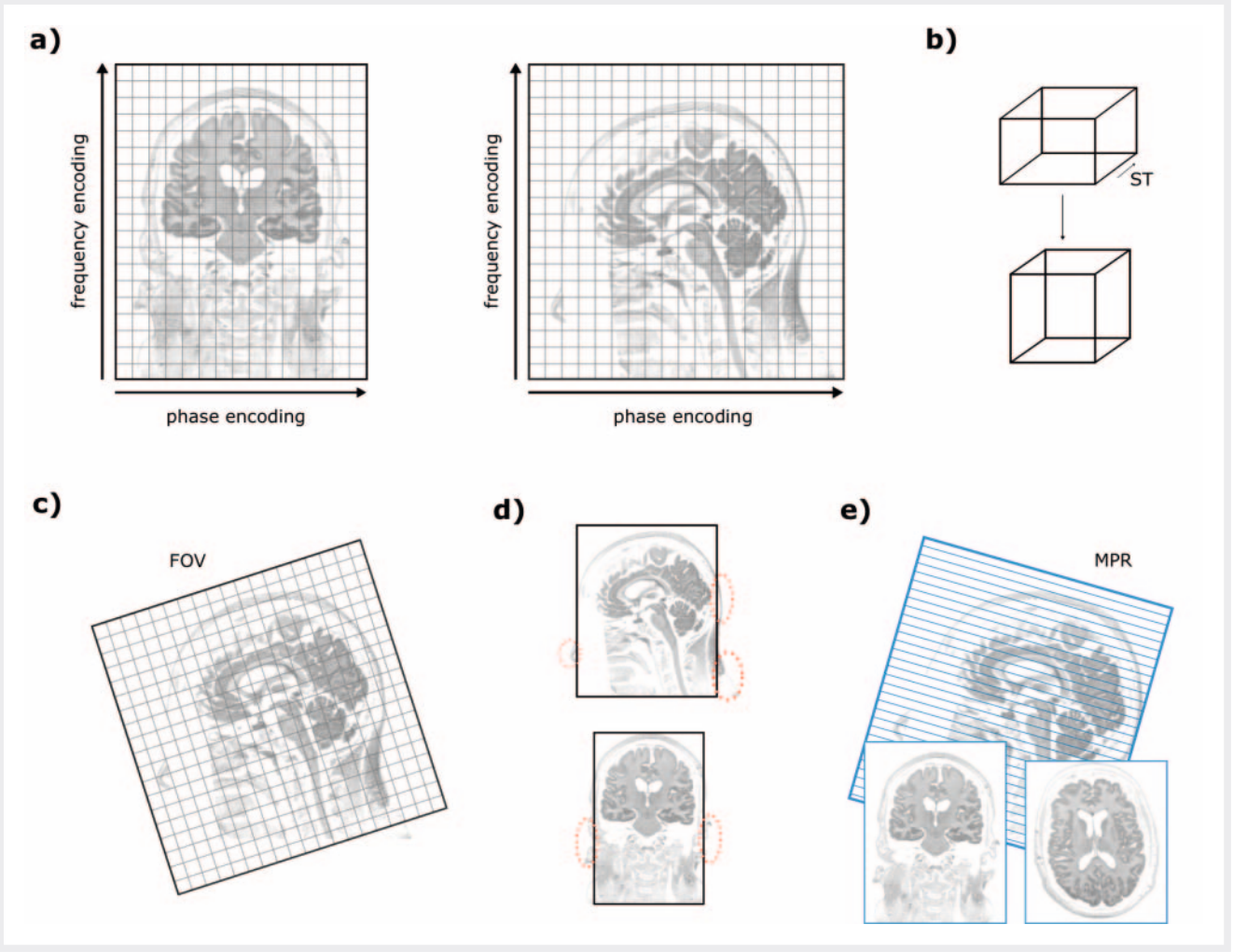

▶ **Fig. 3** Geometric aspects of using whole brain 3D sequences (e. g. 3D FLAIR). **a** A sagittal primary slice orientation is often more efficient and helps to avoid fold-over artefacts due to the lower number of necessary phase-encode steps. **b** Some manufacturers' presets adopt slightly anisotropic voxel dimensions (three different edge lengths, especially higher slice thickness, ST) in order to reduce acquisition time by fewer phase encode steps. Most of these images will, however, be viewed as transverse and coronal reconstructions. Thus, fully or near-isotropic voxels (equal edge lengths) are favourable. A few adjustments of acquisition geometry by the user are thus recommended to achieve isotropic voxels. Additionally, slight **c** tilting and **d** size adjustments of the field of view (FOV) and potentially adjustment of standard head positioning may be necessary in order to both avoid fold-over artefacts and be time efficient. Such artefacts might result in pseudo-lesions, for example caused by a fold-over of the external ears into the brainstem when using parallel imaging techniques in image space (e. g. SENSE). It is recommended to carry out such adjustments as a systematic optimisation instead of adjustments for individual patients. This can help leverage the benefits of such 3D sequences for comparability and automated image analyses. **e** A standardised approach for creating multiplanar reconstructions (MPR) is favourable.

T1-weighted radial Cartesian sequences exhibit somewhat lower contrast than comparable purely Cartesian acquisition techniques when assessed visually, especially for gadolinium-enhancing structures.

Practical notes on application

The number of spokes in the k-space is an important factor influencing image quality. If too few are chosen, the artefacts mentioned above increase significantly. By varying the number of spokes, it is possible to moderately influence the measurement time and SNR in the sense of non-integer averaging, so that for these sequences primarily the number of spokes should be modified instead of the number of averages. Artefacts also arise from signal contributions from outside the field of view (FOV). Coil elements predominantly located outside the FOV should therefore be deactivated [47]. Transverse slice orientation offers potential advantages.

Reduction of metal and other susceptibility artefacts

Technical background and potential advantages

Metallic implants result in pronounced local magnetic field inhomogeneities. As a consequence – among other effects – the linear relationship between precession frequency and spatial position as the basis of location encoding is disturbed. In addition to full signal cancellations, this results in spatial distortions as well as relat-

ed signal loss and signal accumulation, i. e. dark areas with bright edges. These distortions occur both within the slice in the readout direction and perpendicular to the slice plane [48, 49]. Well-established metal artefact reduction methods (see ▶ **Fig. 4**) include the use of a high receiver bandwidth (corresponding to a low water fat shift, depending on the manufacturer); high resolution (including thin slices), preference for TSE sequences with short echo spacing and parallel imaging; if possible, lower field strength, use of less susceptible fat saturation techniques such as Short Tau Inversion Recovery (STIR) and Dixon if necessary, and possibly rotation of the FOV and phase encoding direction to influence the direction of maximum artefact expansion [48, 50, 51]. These principles were first extended to include specific sequences that reduce susceptibility artefacts within the slice by view angle tilting (VAT, e. g., O-MAR or to some extent in the context of WARP). In this case, an additional gradient is switched in the slice selection direction during the readout. This compensates for distortions that have occurred during slice selection [48, 52]. Furthermore, in recent years, multispectral techniques have been established for clinical application, which additionally reduce artefacts from slice to slice [48–51]. In slice-encoding for metal artefact correction (SEMAC) (▶ **Fig. 5**), usually combined with VAT, additional location coding is performed in the direction of the slice stack by using phase encoding. Consequently spatial errors due to the distorted slice profile can be corrected during image reconstruction [48, 53]. During multiacquisition with variable resonance image combination (MAVRIC), multiple three-dimensional TSE data sets are acquired with discrete shifts in transmit and receive frequencies, from which a complete image is assembled in the course of reconstruction [54]. It should also be mentioned that multi-shot techniques (e. g., RESOLVE) can reduce susceptibility artefacts in diffusion-weighted imaging [55]. However, unlike the previously mentioned techniques, the reduced susceptibility of multi-shot DWI is based only on shortened echo trains compared to single-shot techniques and not on actual correction or suppression of susceptibility artefacts. This offers a selection of well-implemented sequences for most body regions. Further reading: [48, 49]

Possible limitations

Metal artefact reduction sequences exhibit significantly increased measurement time, decreased SNR [48], and increased specific absorption rate (SAR) [49]. It should be noted that the increased SAR for critical implants increases the risk of excessive heating of the implant. However, the prolongation of measurement time can be compensated with modern acceleration techniques, e. g., CS for SEMAC [56] and MAVRIC [57] and simultaneous multislice imaging for RESOLVE DWI [58]. VAT creates a blur in the readout direction [48]. Blurring with specific metal artefact reduction has been cited as an argument to use predominantly only conventional artefact reduction modifications for high-resolution peripheral MR neurography [59] if this can sufficiently reduce the extent of the artefacts.

Practical notes on application

Due to the limitations mentioned above, these sequences should not be used across the board for metallic implants in the study area. Rather, individual sequences of these types can be used selectively to assess details in the immediate area of influence of the artefacts.

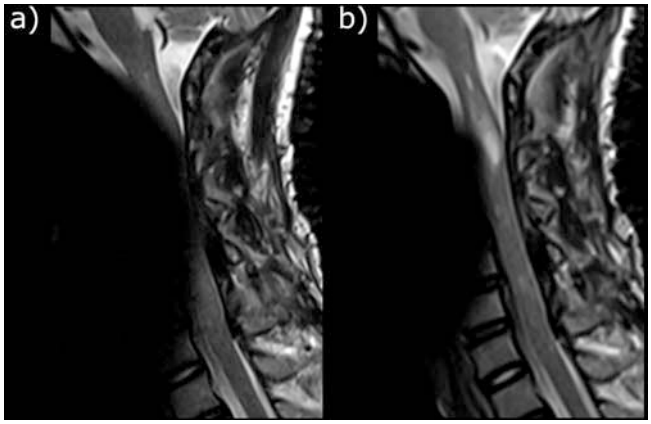

▶ **Fig. 4** Effect of metal artefact reduction on cervical spine imaging in presence of dental braces and material from spinal fusion (outside the image plane): **a** standard T2 TSE with near-total signal loss in the spinal canal at the level of the lesion, **b** T2 TSE with a combination of conventional metal artefact reduction techniques with nearly complete visibility of the spinal cord lesion.

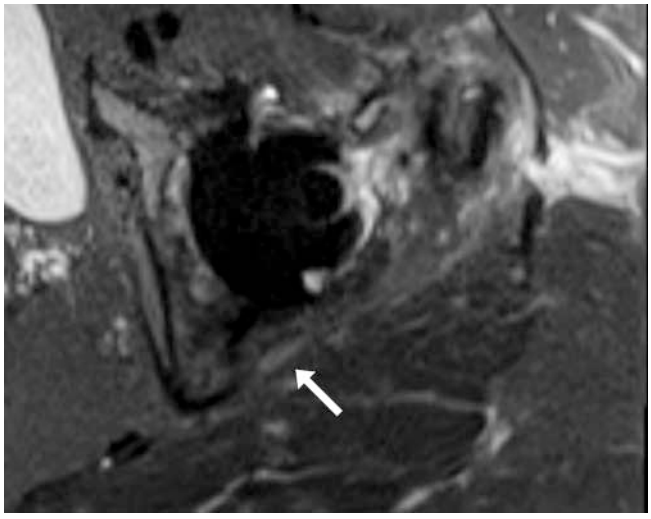

▶ **Fig. 5** 2 D T2 STIR sequence using SEMAC for metal artefact reduction. In this example this technique facilitates assessment of the sciatic nerve (arrow) running immediately dorsal to a hip endoprosthesis.

Dixon Techniques

Technical background and potential advantages

In particular, Dixon techniques (e. g., Dixon, mDixon, IDEAL, Flex, or WFOP) offer relatively homogeneous fat suppression and acquisition of fat-saturated and non-fat-saturated images in a single acquisition. They can be combined with different sequence types (e. g. TSE or gradient echo, 2 D and 3D) and weightings (e. g., T1, T2, PD) and thus used for different targets [30].

Although Dixon techniques were developed as early as the 1980 s and 1990 s [60] and have been refined several times [61–63], they have only found their way into clinical use with newer hardware and software. They use the property that fat and water protons precess at a slightly different frequency [30, 63], so that in-phase and opposed-phase conditions exist depending on the TE. In Dixon techniques, two (or more) partial measurements are made with different echo times. During image reconstruction, pure fat ("F") and water ("W") images can be calculated from this in addition to the in-phase and opposed-phase images. Thus, fat suppression here does not occur as a primary saturation, but by post-processing [30]. Further reading: [30]

Possible limitations

The expected artefacts differ from other fat suppression techniques. A so-called "fat-water swap" is typical: during the computational separation of water and fat signals, it can happen that instead of the water image in image sections or the entire image, the fat signals are actually displayed and vice versa [30, 64]. A partial swap may follow anatomical structures and may then be relatively difficult to detect, most likely with the aid of all calculated image series (▶ **Fig. 6**). Dixon techniques in their pure form are highly susceptible to inhomogeneities of the main magnetic field. However, further developments that determine the present properties of Dixon techniques make them in the end just less susceptible to such magnetic field inhomogeneities [63]. Compared with conventional TSE sequences, Dixon TSE techniques take slightly longer or have slightly worse SNR [30], but can be a very good compromise.

Practical notes on application

Since the individual images to be calculated are typically selected prior to the measurement, it may be useful to calculate all conceivable images from the data, but to maintain clarity, only use the images in the PACS that are primarily relevant for the findings (e. g., in-phase and water image). The Dixon technique can be combined with different sequences and weightings. Consequently image contrast varies greatly with Dixon techniques. Also, artefacts that occur are usually more due to the base sequence than to the Dixon module.

Dixon techniques are most suitable for anatomic transition areas (e. g., neck/thorax [65–67]) and regions adjacent to air-containing spaces (e. g., orbit [26]). They are also relatively robust around metallic implants, although STIR remains superior here [30]. However, STIR fat suppression is based on the short T1 time of fat and therefore can also suppress fat-free lesions after contrast uptake [68], in contrast, fat suppression using the DIXON technique has the advantage that it is based on the frequency difference between water and fat and is independent of T1. T2-weighted Dixon techniques with 2 D TSE sequences can replace STIR in many cases while exhibiting better SNR [30].

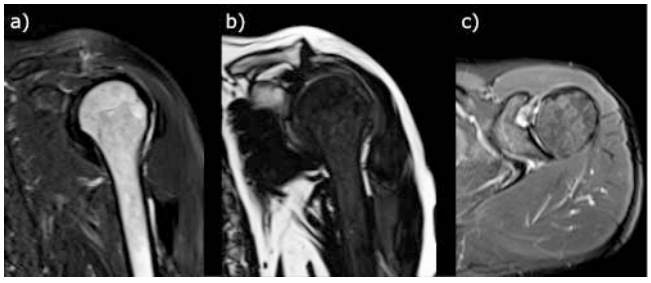

▶ **Fig. 6** Swap artefact in a T2 TSE sequence with Dixon technique. This example shows a misassignment of tissues in parts of the images during image reconstruction. Bone marrow signal of the humerus (indeed fatty) wrongly appears hyperintense in the actual water image **a**, yet hypointense in the actual fat image **b**. The artefact can be suspected because tissue immediately lateral to the humerus features altered signal characteristics as well with an unexpectedly sharp border. An additional T2 STIR sequence **c** unambiguously identifies this as an artefact. This example shows that swap artefacts can follow anatomical boundaries in rare cases. More frequently, however, they affect the entire image or punched out image areas near susceptibility artefacts.

Conclusions

3D techniques allow the creation of multiplanar reconstructions and improve the detectability of small lesions. They are a prerequisite for structured measurements including automated evaluation procedures. In particular, newer 3D TSE techniques such as 3D FLAIR and 3D T1w TSE for vessel wall imaging are now suitable for routine clinical use. Methods for reducing motion and metal artefacts are subject to continuous development. Dixon techniques allow homogeneous fat suppression. Further techniques and implications for different parts of the nervous system will be discussed in a second part of this article.

Conflict of Interest

Christian Mathys: Consulting and lecturing for Siemens on behalf of the employer (Evangelisches Krankenhaus Oldenburg).
The other authors declare that they have no conflict of interest.

References

[1] Rovira A, Wattjes MP, Tintore M et al. Evidence-based guidelines: MAGNIMS consensus guidelines on the use of MRI in multiple sclerosis-clinical implementation in the diagnostic process. Nat Rev Neurol 2015; 11: 471–482. doi:10.1038/nrneurol.2015.106

[2] Filippi M, Preziosa P, Banwell BL et al. Assessment of lesions on magnetic resonance imaging in multiple sclerosis: practical guidelines. Brain 2019; 142: 1858–1875. doi:10.1093/brain/awz144

[3] Traboulsee A, Simon JH, Stone L et al. Revised Recommendations of the Consortium of MS Centers Task Force for a Standardized MRI Protocol and Clinical Guidelines for the Diagnosis and Follow-Up of Multiple Sclerosis. AJNR Am J Neuroradiol 2016; 37: 394–401. doi:10.3174/ajnr.A4539

[4] Ellingson BM, Bendszus M, Boxerman J et al. Consensus recommendations for a standardized Brain Tumor Imaging Protocol in clinical trials. Neuro Oncol 2015; 17: 1188–1198. doi:10.1093/neuonc/nov095

[5] Kaufmann TJ, Smits M, Boxerman J et al. Consensus recommendations for a standardized brain tumor imaging protocol for clinical trials in brain

metastases. Neuro Oncol 2020; 22: 757–772. doi:10.1093/neuonc/noaa030

[6] Wattjes MP, Ciccarelli O, Reich DS et al. 2021 MAGNIMS-CMSC-NAIMS consensus recommendations on the use of MRI in patients with multiple sclerosis. Lancet Neurol 2021; 20: 653–670. doi:10.1016/S1474-4422(21)00095-8

[7] Viallon M, Cuvinciuc V, Delattre B et al. State-of-the-art MRI techniques in neuroradiology: principles, pitfalls, and clinical applications. Neuroradiology 2015; 57: 441–467. doi:10.1007/s00234-015-1500-1

[8] Mugler JP 3rd. Optimized three-dimensional fast-spin-echo MRI. J Magn Reson Imaging 2014; 39: 745–767. doi:10.1002/jmri.24542

[9] Hennig J, Nauerth A, Friedburg H. RARE imaging: a fast imaging method for clinical MR. Magn Reson Med 1986; 3: 823–833. doi:10.1002/mrm.1910030602

[10] Chagla GH, Busse RF, Sydnor R et al. Three-dimensional fluid attenuated inversion recovery imaging with isotropic resolution and nonselective adiabatic inversion provides improved three-dimensional visualization and cerebrospinal fluid suppression compared to two-dimensional flair at 3 tesla. Invest Radiol 2008; 43: 547–551. doi:10.1097/RLI.0b013e3181814d28

[11] Kallmes DF, Hui FK, Mugler JP et al. Suppression of cerebrospinal fluid and blood flow artifacts in FLAIR MR imaging with a single-slab three-dimensional pulse sequence: initial experience. Radiology 2001; 221: 251–255. doi:10.1148/radiol.2211001712

[12] Saranathan M, Worters PW, Rettmann DW et al. Physics for clinicians: Fluid-attenuated inversion recovery (FLAIR) and double inversion recovery (DIR) Imaging. J Magn Reson Imaging 2017; 46: 1590–1600. doi:10.1002/jmri.25737

[13] Kakeda S, Korogi Y, Hiai Y et al. Pitfalls of 3D FLAIR brain imaging: a prospective comparison with 2D FLAIR. Acad Radiol 2012; 19: 1225–1232. doi:10.1016/j.acra.2012.04.017

[14] Lecler A, Bouzad C, Deschamps R et al. Optimizing 3D FLAIR to detect MS lesions: pushing past factory settings for precise results. J Neurol 2019; 266: 2786–2795. doi:10.1007/s00415-019-09490-y

[15] Lecler A, El Sanharawi I, El Methni J et al. Improving Detection of Multiple Sclerosis Lesions in the Posterior Fossa Using an Optimized 3D-FLAIR Sequence at 3T. AJNR Am J Neuroradiol 2019; 40: 1170–1176. doi:10.3174/ajnr.A6107

[16] Polak P, Magnano C, Zivadinov R et al. 3D FLAIRED: 3D fluid attenuated inversion recovery for enhanced detection of lesions in multiple sclerosis. Magn Reson Med 2012; 68: 874–881. doi:10.1002/mrm.23289

[17] Algin O, Turkbey B. Evaluation of aqueductal stenosis by 3D sampling perfection with application-optimized contrasts using different flip angle evolutions sequence: preliminary results with 3T MR imaging. AJNR Am J Neuroradiol 2012; 33: 740–746. doi:10.3174/ajnr.A2833

[18] Levy LM, Di Chiro G, Brooks RA et al. Spinal cord artifacts from truncation errors during MR imaging. Radiology 1988; 166: 479–483. doi:10.1148/radiology.166.2.3336724

[19] Lindenholz A, van der Kolk AG, Zwanenburg JJM et al. The Use and Pitfalls of Intracranial Vessel Wall Imaging: How We Do It. Radiology 2018; 286: 12–28. doi:10.1148/radiol.2017162096

[20] Leao DJ, Agarwal A, Mohan S et al. Intracranial vessel wall imaging: applications, interpretation, and pitfalls. Clin Radiol 2020; 75: 730–739. doi:10.1016/j.crad.2020.02.006

[21] Zhu C, Tian B, Chen L et al. Accelerated whole brain intracranial vessel wall imaging using black blood fast spin echo with compressed sensing (CS-SPACE). MAGMA 2018; 31: 457–467. doi:10.1007/s10334-017-0667-3

[22] Guggenberger K, Krafft AJ, Ludwig U et al. High-resolution Compressed-sensing T1 Black-blood MRI: A New Multipurpose Sequence in Vascular Neuroimaging? Clin Neuroradiol 2019. doi:10.1007/s00062-019-00867-0

[23] Park CJ, Cha J, Ahn SS et al. Contrast-Enhanced High-Resolution Intracranial Vessel Wall MRI with Compressed Sensing: Comparison with Conventional T1 Volumetric Isotropic Turbo Spin Echo Acquisition Sequence. Korean J Radiol 2020; 21: 1334–1344. doi:10.3348/kjr.2020.0128

[24] Okuchi S, Fushimi Y, Okada T et al. Visualization of carotid vessel wall and atherosclerotic plaque: T1-SPACE vs. compressed sensing T1-SPACE. Eur Radiol 2019; 29: 4114–4122. doi:10.1007/s00330-018-5862-8

[25] Cho SJ, Jung SC, Suh CH et al. High-resolution magnetic resonance imaging of intracranial vessel walls: Comparison of 3D T1-weighted turbo spin echo with or without DANTE or iMSDE. PLoS One 2019; 14: e0220603. doi:10.1371/journal.pone.0220603

[26] Riederer I, Sollmann N, Muhlau M et al. Gadolinium-Enhanced 3D T1-Weighted Black-Blood MR Imaging for the Detection of Acute Optic Neuritis. AJNR Am J Neuroradiol 2020. doi:10.3174/ajnr.A6807

[27] Mugler JP 3rd, Brookeman JR. Three-dimensional magnetization-prepared rapid gradient-echo imaging (3D MP RAGE). Magn Reson Med 1990; 15: 152–157. doi:10.1002/mrm.1910150117

[28] Haacke EM, Xu Y, Cheng YC et al. Susceptibility weighted imaging (SWI). Magn Reson Med 2004; 52: 612–618. doi:10.1002/mrm.20198

[29] Liu S, Buch S, Chen Y et al. Susceptibility-weighted imaging: current status and future directions. NMR Biomed 2017: 30. doi:10.1002/nbm.3552

[30] Guerini H, Omoumi P, Guichoux F et al. Fat Suppression with Dixon Techniques in Musculoskeletal Magnetic Resonance Imaging: A Pictorial Review. Semin Musculoskelet Radiol 2015; 19: 335–347. doi:10.1055/s-0035-1565913

[31] Feng L, Benkert T, Block KT et al. Compressed sensing for body MRI. J Magn Reson Imaging 2017; 45: 966–987. doi:10.1002/jmri.25547

[32] Conklin J, Longo MGF, Cauley SF et al. Validation of Highly Accelerated Wave-CAIPI SWI Compared with Conventional SWI and T2*-Weighted Gradient Recalled-Echo for Routine Clinical Brain MRI at 3T. AJNR Am J Neuroradiol 2019; 40: 2073–2080. doi:10.3174/ajnr.A6295

[33] Pipe JG. Motion correction with PROPELLER MRI: application to head motion and free-breathing cardiac imaging. Magn Reson Med 1999; 42: 963–969. doi:10.1002/(sici)1522-2594(199911)42:5<963::aid-mrm17>3.0.co;2-l

[34] Finkenzeller T, Wendl CM, Lenhart S et al. BLADE Sequences in Transverse T2-weighted MR Imaging of the Cervical Spine. Cut-off for Artefacts? Rofo 2015; 36: 102–108. doi:10.1055/s-0034-1385179

[35] Alibek S, Adamietz B, Cavallaro A et al. Contrast-enhanced T1-weighted fluid-attenuated inversion-recovery BLADE magnetic resonance imaging of the brain: an alternative to spin-echo technique for detection of brain lesions in the unsedated pediatric patient? Acad Radiol 2008; 15: 986–995. doi:10.1016/j.acra.2008.03.009

[36] Mavroidis P, Giankou E, Tsikrika A et al. Brain imaging: Comparison of T1W FLAIR BLADE with conventional T1W SE. Magn Reson Imaging 2017; 37: 234–242. doi:10.1016/j.mri.2016.12.007

[37] Vertinsky AT, Rubesova E, Krasnokutsky MV et al. Performance of PROPELLER relative to standard FSE T2-weighted imaging in pediatric brain MRI. Pediatr Radiol 2009; 39: 1038–1047. doi:10.1007/s00247-009-1292-8

[38] Lavdas E, Mavroidis P, Kostopoulos S et al. Reduction of motion, truncation and flow artifacts using BLADE sequences in cervical spine MR imaging. Magn Reson Imaging 2015; 33: 194–200. doi:10.1016/j.mri.2014.10.014

[39] Zaitsev M, Maclaren J, Herbst M. Motion artifacts in MRI: A complex problem with many partial solutions. J Magn Reson Imaging 2015; 42: 887–901. doi:10.1002/jmri.24850

[40] Glover GH, Pauly JM. Projection reconstruction techniques for reduction of motion effects in MRI. Magn Reson Med 1992; 28: 275–289. doi:10.1002/mrm.1910280209

[41] Lee S-J, Yu S-M. The image evaluation of iterative motion correction reconstruction algorithm PROPELLER T2-weighted imaging compared with MultiVane T2-weighted imaging. Journal of the Korean Physical Society 2017; 71: 238–243. doi:10.3938/jkps.71.238

[42] Bangiyev L, Raz E, Block TK et al. Evaluation of the orbit using contrast-enhanced radial 3D fat-suppressed T1 weighted gradient echo (Radial-VIBE) sequence. Br J Radiol 2015; 88: 20140863. doi:10.1259/bjr.20140863

[43] Wu X, Raz E, Block TK et al. Contrast-enhanced radial 3D fat-suppressed T1-weighted gradient-recalled echo sequence versus conventional fat-suppressed contrast-enhanced T1-weighted studies of the head and neck. Am J Roentgenol 2014; 203: 883–889. doi:10.2214/Am J Roentgenol.13.11729

[44] Chandarana H, Block KT, Winfeld MJ et al. Free-breathing contrast-enhanced T1-weighted gradient-echo imaging with radial k-space sampling for paediatric abdominopelvic MRI. Eur Radiol 2014; 24: 320–326. doi:10.1007/s00330-013-3026-4

[45] Chandarana H, Block TK, Rosenkrantz AB et al. Free-breathing radial 3D fat-suppressed T1-weighted gradient echo sequence: a viable alternative for contrast-enhanced liver imaging in patients unable to suspend respiration. Invest Radiol 2011; 46: 648–653. doi:10.1097/RLI.0b013e31821eea45

[46] Hedderich DM, Weiss K, Spiro JE et al. Clinical Evaluation of Free-Breathing Contrast-Enhanced T1w MRI of the Liver using Pseudo Golden Angle Radial k-Space Sampling. Rofo 2018; 190: 601–609. doi:10.1055/s-0044-101263

[47] Xue Y, Yu J, Kang HS et al. Automatic coil selection for streak artifact reduction in radial MRI. Magn Reson Med 2012; 67: 470–476. doi:10.1002/mrm.23023

[48] Dillenseger JP, Moliere S, Choquet P et al. An illustrative review to understand and manage metal-induced artifacts in musculoskeletal MRI: a primer and updates. Skeletal Radiol 2016; 45: 677–688. doi:10.1007/s00256-016-2338-2

[49] Talbot BS, Weinberg EP. MR Imaging with Metal-suppression Sequences for Evaluation of Total Joint Arthroplasty. Radiographics 2016; 36: 209–225. doi:10.1148/rg.2016150075

[50] Khodarahmi I, Isaac A, Fishman EK et al. Metal About the Hip and Artifact Reduction Techniques: From Basic Concepts to Advanced Imaging. Semin Musculoskelet Radiol 2019; 23: e68–e81. doi:10.1055/s-0039-1687898

[51] Jungmann PM, Agten CA, Pfirrmann CW et al. Advances in MRI around metal. J Magn Reson Imaging 2017; 46: 972–991. doi:10.1002/jmri.25708

[52] Cho ZH, Kim DJ, Kim YK. Total inhomogeneity correction including chemical shifts and susceptibility by view angle tilting. Med Phys 1988; 15: 7–11. doi:10.1118/1.596162

[53] Lu W, Pauly KB, Gold GE et al. SEMAC: Slice Encoding for Metal Artifact Correction in MRI. Magn Reson Med 2009; 62: 66–76. doi:10.1002/mrm.21967

[54] Koch KM, Lorbiecki JE, Hinks RS et al. A multispectral three-dimensional acquisition technique for imaging near metal implants. Magn Reson Med 2009; 61: 381–390. doi:10.1002/mrm.21856

[55] Porter DA, Heidemann RM. High resolution diffusion-weighted imaging using readout-segmented echo-planar imaging, parallel imaging and a two-dimensional navigator-based reacquisition. Magn Reson Med 2009; 62: 468–475. doi:10.1002/mrm.22024

[56] Fritz J, Ahlawat S, Demehri S et al. Compressed Sensing SEMAC: 8-fold Accelerated High Resolution Metal Artifact Reduction MRI of Cobalt-Chromium Knee Arthroplasty Implants. Invest Radiol 2016; 51: 666–676. doi:10.1097/RLI.0000000000000317

[57] Worters PW, Sung K, Stevens KJ et al. Compressed-sensing multispectral imaging of the postoperative spine. J Magn Reson Imaging 2013; 37: 243–248. doi:10.1002/jmri.23750

[58] Frost R, Jezzard P, Douaud G et al. Scan time reduction for readout-segmented EPI using simultaneous multislice acceleration: Diffusion-weighted imaging at 3 and 7 Tesla. Magn Reson Med 2015; 74: 136–149. doi:10.1002/mrm.25391

[59] Ahlawat S, Stern SE, Belzberg AJ et al. High-resolution metal artifact reduction MR imaging of the lumbosacral plexus in patients with metallic implants. Skeletal Radiol 2017; 46: 897–908. doi:10.1007/s00256-017-2630-9

[60] Dixon WT. Simple proton spectroscopic imaging. Radiology 1984; 153: 189–194. doi:10.1148/radiology.153.1.6089263

[61] Glover GH, Schneider E. Three-point Dixon technique for true water/fat decomposition with B0 inhomogeneity correction. Magn Reson Med 1991; 18: 371–383. doi:10.1002/mrm.1910180211

[62] Hardy PA, Hinks RS, Tkach JA. Separation of fat and water in fast spin-echo MR imaging with the three-point Dixon technique. J Magn Reson Imaging 1995; 5: 181–185. doi:10.1002/jmri.1880050213

[63] Ma J. Dixon techniques for water and fat imaging. J Magn Reson Imaging 2008; 28: 543–558. doi:10.1002/jmri.21492

[64] Romu T, Dahlstrom N, Leinhard OD et al. Robust water fat separated dual-echo MRI by phase-sensitive reconstruction. Magn Reson Med 2017; 78: 1208–1216. doi:10.1002/mrm.26488

[65] Gaddikeri S, Mossa-Basha M, Andre JB et al. Optimal Fat Suppression in Head and Neck MRI: Comparison of Multipoint Dixon with 2 Different Fat-Suppression Techniques, Spectral Presaturation and Inversion Recovery, and STIR. AJNR Am J Neuroradiol 2018; 39: 362–368. doi:10.3174/ajnr.A5483

[66] Wendl CM, Eiglsperger J, Dendl LM et al. Fat suppression in magnetic resonance imaging of the head and neck region: is the two-point DIXON technique superior to spectral fat suppression? Br J Radiol 2018; 91: 20170078. doi:10.1259/bjr.20170078

[67] Ma J, Jackson EF, Kumar AJ et al. Improving fat-suppressed T2-weighted imaging of the head and neck with 2 fast spin-echo dixon techniques: initial experiences. AJNR Am J Neuroradiol 2009; 30: 42–45. doi:10.3174/ajnr.A1132

[68] Krinsky G, Rofsky NM, Weinreb JC. Nonspecificity of short inversion time inversion recovery (STIR) as a technique of fat suppression: pitfalls in image interpretation. Am J Roentgenol 1996; 166: 523–526. doi:10.2214/ajr.166.3.8623620